RESEARCH ARTICLE | OCTOBER 07 2011

Electronic states of tetrahydrofuran molecules studied by electron collisions

Mariusz Zubek; Marcin Dampc; Ireneusz Linert; Tomasz Neumann

J. Chem. Phys. 135, 134317 (2011)
https://doi.org/10.1063/1.3646511

Electronic states of tetrahydrofuran molecules studied by electron collisions

Mariusz Zubek,[a] Marcin Dampc, Ireneusz Linert, and Tomasz Neumann
Department of Physics of Electronic Phenomena, Gdańsk University of Technology, 80-233 Gdańsk, Poland

(Received 16 August 2011; accepted 15 September 2011; published online 7 October 2011)

Electronic states of tetrahydrofuran molecules were studied in the excitation energy range 5.5–10 eV using the technique of electron energy loss spectroscopy in the gas phase. Excitation from the two conformations, C_2 and C_s, of the ground state of the molecule are observed in the measured energy loss spectra. The vertical excitation energies of the $^3(n_o3s)$ triplet state from the C_2 and C_s conformations of the ground state of the molecule are determined to be 6.03 ± 0.02 and 6.25 ± 0.02 eV, respectively. The singlet-triplet energy splitting for the n_o3s configuration is determined to be 0.31 eV. It is also found that excitation from the C_s conformation of the ground state has a higher cross section than that from the C_2 conformation. © *2011 American Institute of Physics*. [doi:10.1063/1.3646511]

I. INTRODUCTION

Spectroscopy of the electronic excited states of polyatomic molecules has recently attracted considerable attention because of the role the states play in molecular decay processes following photon and electron impact.[1] In heterocyclic five-membered hydrocarbon molecules, excitation to lower excited states initiates non-radiative deactivation processes which lead to molecular dissociation. For example, in the photodissociation reactions in furan, excitation to lower lying states, $^1\pi\pi^*$ and $^1\pi 3p$, leads to formation of molecular fragments directly on the potential energy surface and also through internal conversion involving conical intersections between the excited and ground states.[2,3] In the electron impact excitation of the hydrocarbon molecules, the excited valence and Rydberg states act as parent states of core-excited negative-ion resonances. The dissociative electron attachment above 5 eV in furan proceeds via a core-excited resonance, which in a complex molecular reaction decays into various fragment ions.[4] Moreover, accurate data on energies and symmetries of the excited states of the polyatomic molecules are required for the theoretical studies of the inelastic electron collisions to predict the positions of these negative-ion resonances. The spectroscopic data on the excited states are routinely gained from vacuum ultraviolet absorption measurements, which, although having high energy resolution, are limited to the optically allowed states. Electron collision spectroscopy extends these data to include the optically forbidden (triplet) states and extends the understanding of the complexity of the valence and Rydberg states and their interactions in the polyatomic molecules.

In the present study, the electronic excited states of tetrahydrofuran (THF) molecules were studied by electron impact energy loss spectroscopy. The THF molecule, C_4H_8O, is a five-membered heterocyclic compound, which may be considered as a hydrogenated form of furan. In the last decade, THF has become a subject of extensive research in high-energy radiation damage of living cells. It is regarded to be the elementary prototype of deoxyribose, the DNA structural unit, which links the phosphate group and the nuclei bases. It is now well established that the secondary electrons, which are produced in large quantities by the primary ionizing particles in the biological material, may cause single- and double-strand breaks in the polynucleotides of DNA through site selective cleavage of the molecular bonds.[5] The molecular bonds are cleaved very efficiently through dissociative electron attachment, dissociative ionization, and dissociative excitation. In the last process, excited states are involved, which dissociate producing neutral fragments and radicals. Spectroscopic studies of these excited states support elucidation of the dissociation processes.

The electronic states of THF were initially investigated by applying vacuum ultraviolet (VUV) absorption spectroscopy.[6–9] Recently, Bremner *et al.*[10] obtained VUV spectra of THF at a resolution of 0.2 nm in the 5.8–11.0 eV energy region, which is in good agreement with the earlier published results.[8,9] The absorption bands observed at 6.6, 7.20, 7.82, 8.57, and 8.89 eV were assigned to the n_o3s, n_o3p, n_o3d, n_o4p, and n_o5p excited states, respectively. These states correspond to excitation of the oxygen non-bonding electron n_o from the HOMO orbital to the Rydberg orbitals. More recently, Giuliani *et al.*[11] measured the photoabsorption spectra of THF with higher resolution, of approximately 0.075 nm, in the 5.8–10.6 eV energy region and also performed high-level *ab initio* calculations on the excited states of the THF molecule. Their experimental results appeared to be in very good agreement with the data of Bremner *et al.*[10] However, the excellent agreement between the results of the calculations and the measurements demonstrated that the observed VUV absorption spectrum contains electronic bands corresponding to excitation from the twisted C_s and envelope C_2 conformers of the ground state of THF. These conformers are populated alternatively in the pseudorotation

[a]Electronic mail: mazub@mif.pg.gda.pl.

motion of the molecule, which is a vibrational motion with a puckering deformation that occurs out of the plane of the molecule.[12] Giuliani *et al*., in a Boltzmann analysis at 298 K, estimated that the C_s and C_2 conformers are simultaneously populated with the rates of 55.5% and 44.5%, respectively. Following this finding, they re-examined the absorption electronic bands and assigned them to transitions into the Rydberg states within the respective C_s and C_2 conformers. For example, they showed that the first absorption band of the n_o3s excited state contains two sub-bands with calculated vertical excitation energies of 6.357 and 6.608 eV due to transitions from the C_2 and C_s conformers of the ground state of THF, respectively. The transition from the C_s conformer had higher intensity than that from the C_2 conformer.

The first electron impact energy loss spectrum of THF molecules in the gas phase was reported by Tam and Brion.[13] They carried out measurements at an incident energy of 100 eV and a scattering angle of 2°, which favor the dipole allowed transitions. The first three energy loss peaks have energies that coincide with those of the VUV spectra and were assigned to transitions into the 3s, 3p, and 3d Rydberg states from a comparison with photoelectron spectra. The near-threshold electron energy loss measurements were performed by Bremner *et al*.[10] Their energy loss spectrum at electron residual energy of ≈0.3 eV showed a broadband with a maximum between 6.3 and 6.5 eV, which shifted to higher energies with increasing residual energy and had the appearance of resonance excitation processes of the triplet and singlet states. Very recently electron energy loss spectra were obtained by Do *et al*.[14] in their work on measurements of the differential cross sections of the three lowest bands of electronic states of THF in the impact energy range 15–50 eV. In the condensed phase of deposited thin film layers of THF, high-resolution electron energy loss spectra of Antic *et al*.[15] showed several overlapping excited bands of THF in the region 6–9.5 eV. Finally, calculations of energies of the triplet and singlet excited states of THF were carried out by Bouchiha *et al*.[16] using the HF-SCF pseudo-natural orbitals in the R-matrix studies of the electronically inelastic cross sections for electron scattering from THF.

In the present work, energy loss spectra were measured in THF in the excitation energy range 5.5–10 eV at constant electron residual energies E_r which varied from 0.02 eV to 10 eV. The measurements were carried out using a crossed electron-molecular beam spectrometer, which for measurements in the region of the threshold and near-threshold excitation was modified to implement the penetrating field technique. This technique enabled the location and observation of excitation of the triplet $^3(n_o3s)$ Rydberg state of the THF molecule. The present studies also allows the identification of the electronic excitation of THF from the C_2 and C_s conformers of the ground electronic state and indicates that transitions from the C_s conformer have higher excitation cross sections. This work was motivated by the present need for more accurate spectroscopic data on the electronic states of THF, which is considered as an elementary prototype of deoxyribose.

II. EXPERIMENTAL

The electron spectrometer employed in the present measurements combines a source of a monochromatized electron beam and a scattered electron analyzer. The incident electron beam is scattered from the target gas beam. The energy-selected electrons leaving the double hemispherical selector of the monochromator are focused at the gas beam by a triple-electrode cylindrical lens. The scattered electron analyzer, which incorporates a decelerating triple-electrode cylindrical lens and a double hemispherical selector, both of which are identical to that used in the monochromator, can be rotated about the target beam axis. The molecular beam is produced by effusion of the target compound vapour from a single capillary of 0.6 mm inner diameter. The scattering angle was calibrated against the positions of minima in the elastic electron scattering from argon[17] with an uncertainty of ±1.5°. The incident electron energy scale was determined by monitoring the position of the ^2S negative ion resonance in helium at 19.365 eV[18] with an uncertainty of ±20 meV. The overall energy resolution of the spectrometer working in the energy loss mode, for the constant electron residual energy $E_r > 2$ eV, was about 90 meV (FWHM), which stemmed from an increased pass energy of the selector in the monochromator. This was required to obtain higher incident beam current and to gain sufficiently high scattered electron intensities. These intensities were, in general, low, for example, equal to about 3.5 Hz at the first energy loss peak of the spectrum in Fig. 4(b), due to low values of the electronic excitation cross sections of THF. The low values of the cross sections were confirmed very recently by the absolute measurements of Do *et al*.[14]

The spectrometer, which has been described in detail elsewhere,[19] incorporated a magnetic angle changer used in our previous studies over the extended scattering angle range 20°–180°. However, for the purpose of this work it was removed and the spectrometer was further substantially modified. In this modification, the deceleration cylindrical lens of the electron analyzer was rebuild to insert the extracting electrode (see below), which allowed the implementation of the penetrating electrostatic field technique.[20,21] This technique enabled the detection, with high efficiency, of low energy threshold electrons produced in the excitation of the target molecules. In addition, to provide a tool for estimating possible contributions of any negative ions, produced in the collision region with low kinetic energies, into the threshold electron spectra a magnetic field deflector was introduced into the spectrometer. It was placed between the exit of the hemispherical selector in the electron analyzer and the electron channel multiplier.

The modified design of the electron analyzer input lens is shown in Fig. 1(a). The extracting electrode, maintained at a potential of 80–100 V, is placed between the entrance electrode of the cylindrical lens and the shield, which is kept at a ground potential. The electrostatic field, from the region between the extracting electrode and the shield penetrates through an opening into the collision region, as shown in Fig. 1(a). A weak electrostatic field is produced at the collision region, which collects very low energy electrons with

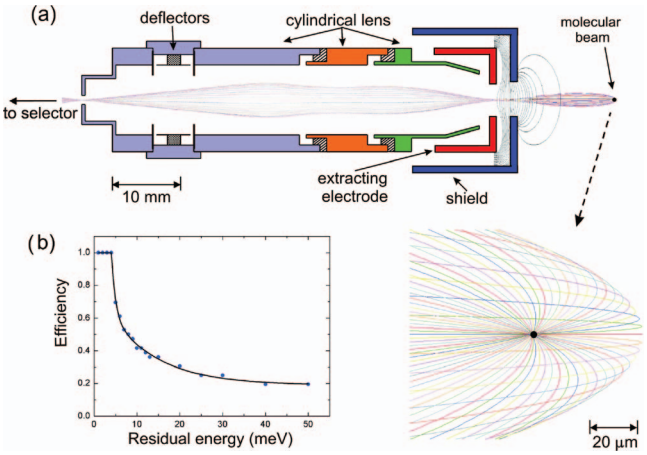

FIG. 1. (a) Diagram of the entrance lens of the electron analyzer modified to implement the penetrating electrostatic field technique. Shown are trajectories of electrons of 1 meV kinetic energy generated in the collision region and the shape of the penetrating electrostatic field in the region of the entrance to the electron analyzer. (b) Collection efficiency in the penetrating field technique of the entrance lens of the electron analyzer calculated as a function of the electron energy.

high efficiency over a large solid angle. Figure 1(a) and the inset, on an enlarged scale, show trajectories of threshold electrons having 1 meV kinetic energy, calculated using the charge particle optics CPO computer program.[23] The inset clearly indicates electron collection from a complete solid angle of 4π at this energy. These electrons are focused in the region between the extracting electrode and the shield and from that point are further transmitted by the cylindrical lens onto the entrance aperture of the hemispherical selector (Fig. 1(a)). The total collection efficiency of the combined extraction stage and the cylindrical lens focusing electrons, calculated using the CPO computer program,[23] is displayed as a function of electron energy in Fig. 1(b). The efficiency is constant and equal to 100% for electron energies up to 4 meV, and above 4 meV it decreases fast with increasing energy, as a result of decreasing solid angle of collection of the extraction stage, as found previously in Ref. 20. The double hemispherical selector of the analyzer transmits to the detector electrons with energies controlled by the residual energy voltage on the electron analyzer.

The performance of the electron analyzer working in the penetrating field mode for $E_r < 0.03$ eV was tested by measuring the threshold excitation spectra of helium and recording the relative intensities of the 2^3S and 2^1S threshold peaks. The ratio of the 2^1S to 2^3S peaks, as noted before,[20] depends on the residual energy of the collected electrons and the obtained peak ratio may be taken as a measure of the residual energy. For example, our highest peak ratio of 2.5 corresponds[24] to residual energy $E_r = 0.02$ eV. In the operation of the spectrometer in the penetrating field mode but for higher residual energies 0.05–0.25 eV (non-threshold mode), the E_r values were found from the electron energy loss and the known incident electron energy. The electron energy loss scale was calibrated against the position of the 2^1S excitation peak at 20.615 eV to within ±20 meV. The overall energy resolution of the spectrometer in these measurements was about 70 meV (FWHM).

The magnetic field deflector built to separate electrons from the negative ions, which may be produced in the collision region and detected simultaneously consists of two small coils of 1 cm diameter, each having 4 layers of 10 turns of copper wire. The construction of the deflector followed the design principle first described in Ref. 22. These coils generate a magnetic field, which deflects particles with equal charge and energy according to the square root of their masses. The field is perpendicular to motion of the charged particles. It has been seen using the CPO computer simulations that a magnetic field of 10 G corresponding to 0.5 A current in the coils removes 5 eV electrons from the beam, whereas the negative ions of mass 20 amu and higher reach the channel electron multiplier with unaltered intensity. The operation of the deflector was tested by recording the threshold spectra in carbon monoxide, which, in the energy range 9.5–10.6 eV, contain peaks due to the threshold electrons from excitation of the $b^3\Sigma^+$ state and low energy (∼0.1 eV) oxygen negative ions.[25]

The anhydrous liquid THF was placed in a stainless steel container attached to a gas line which was maintained at the room temperature. Heating of the sample was not required as the THF has sufficiently high vapour pressure at this temperature. It was degassed several times under low pressure to remove contaminating gases, nitrogen, oxygen, and water vapour, before introducing into the spectrometer by a leak valve, which was heated to avoid THF condensation. THF were purchased from Sigma-Aldrich Chemie with a stated purity of 99.9%.

III. RESULTS AND DISCUSSION

The electron energy loss spectra obtained in THF at the increasing constant residual electron energies E_r of 0.02, 0.05, 0.16, and 0.24 eV are presented in Fig. 2. It was verified by using the magnetic field deflector that the possible contribution of the negative ions, formed in the dissociative electron attachment to THF molecule into the above spectra is below 3%. The $E_r = 0.02$ eV spectrum (Fig. 2(a)) displays a broad maximum peaking at 6.25 eV. Above this maximum, the scattered electron intensity rises smoothly with increasing electron energy loss. There are two shoulders noticeable on the low energy slope of the maximum and a wider although weak energy loss structure discernible at 8.1 eV on the rising electron intensity. This rising background corresponds to excitation of a number of excited states of THF, which may include dissociating states that are not resolved as individual excitation bands. Spectra measured at $E_r = 0.02$ eV in the 3.0–5.7 eV incident electron energy range (not shown in Fig. 2(a)) did not indicate inelastic electron scattering, detected above the noise background, which was equal to 0.5%–1% of the intensity of the 6.25 eV peak. The spectrum measured at the $E_r = 0.05$ eV (Fig. 2(b)) begins with a broad maximum at 6.30 eV, having a similar shape to that of the 0.02 eV spectrum. Above 6.9 eV, the electron intensity varies indicating at least two wider energy loss bands of excited states of THF superimposed on a rising background. The first maximum in the third spectrum (Fig. 2(c)) measured at $E_r = 0.16$ eV is further shifted to

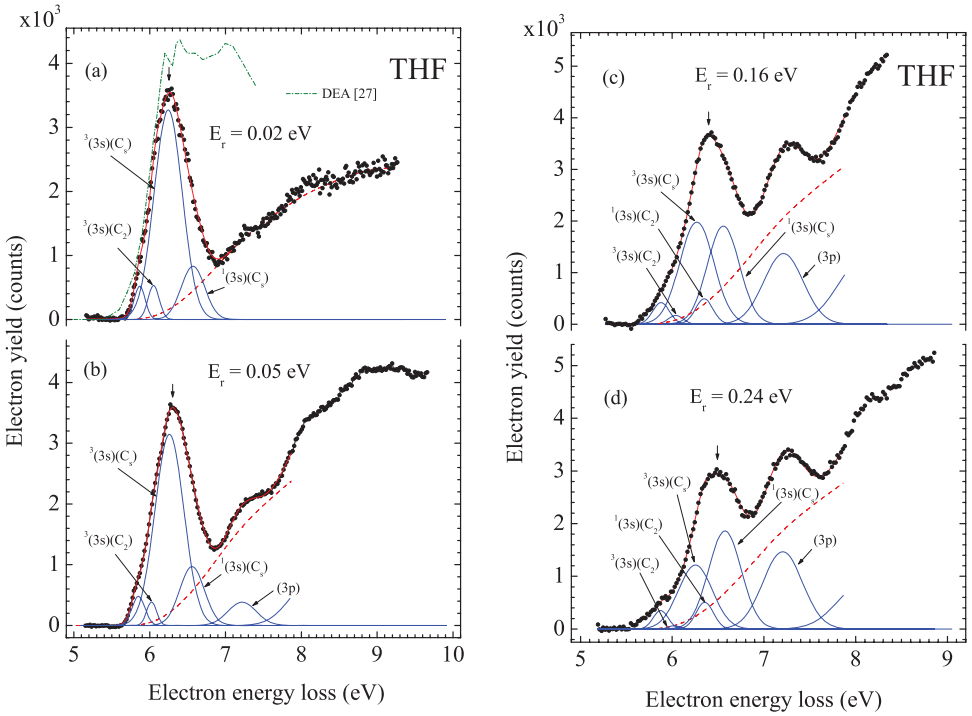

FIG. 2. Electron energy loss spectra measured in THF for constant residual energy E_r of: (a) 0.02 eV, (b) 0.05 eV, (c) 0.16 eV, and (d) 0.24 eV. Also shown are (full lines) bands fitted to the experimental spectra and their final fits and the approximated (dashed lines) unresolved inelastic electron background. The assignments of the excitation bands are shown for the C_2 and C_s conformations of the ground electronic state of THF. (a) The dissociative electron attachment band (dashed-dotted line) for $C_2H_3O^-$ negative ion from Ref. 27 (as read from their Fig. 3).

6.40 eV, while the onset of the spectrum is moved down to lower energy by about 0.10 eV. The subsequent excitation band is now clearly visible and has higher relative intensity than in the previous spectrum of Fig. 2(b). Its maximum is placed at 7.21 eV. Finally, energy loss spectrum obtained at the $E_r = 0.24$ eV shows the first maximum at 6.50 eV and has an onset at 5.50 eV, while its oval shape plainly indicates contribution of at least two excitation bands.

The variation of positions and shapes of the first broad maxima with increasing electron residual energy in the energy loss spectra of Fig. 2 points at a contribution of several states of THF, which have excitation cross sections that vary drastically with energy in the threshold and near-threshold regions. To resolve the excitation bands in the measured spectra, they were fitted with Gaussian profiles and the band profiles giving the best fits are shown in Fig. 2 together with the overall fit to the measured spectra. Because this is a nonlinear regression problem, the used fitting procedure started with a single Gaussian profile to describe the main peak of the spectrum and in each next iteration the number of the applied profiles was increased by one. The fitting was stopped when the overall fit to the measured spectrum gave satisfactory agreement for a given, the lowest, number of profiles. Further increase in the number of profiles did not improve the obtained overall fit. In this fitting, the contributions of the unresolved inelastic electron intensities (the rising background) were approximated by a smoothly varying function, as shown by the dashed lines in Fig. 2. It is of note that the fitting procedure gave a very satisfactory agreement simultaneously for the four experimental spectra implementing excitation bands, whose positions and widths were consistent to within $\pm$ 0.02 eV.

The fitting of the broad peak in the spectrum of Fig. 2(a) indicates excitation of four bands having vertical excitation energies at 5.87, 6.03, 6.25, and 6.56 eV. The energy of the 6.56 eV band is in very good agreement with that found for excitation of the singlet $^1(n_o3s)$ state of the THF from the C_s conformation by Giulliani *et al.*[11] in their VUV absorption studies. It is also in excellent agreement with our energy loss spectrum measured at $E_r = 10.0$ eV and $\Theta = 0^\circ$ (see below), which favors excitation of the optically allowed states. Thus, we assign this band to excitation of the singlet, Rydberg $^1(n_o3s)$ state from the C_s conformation of the THF molecule. The 6.25 and 6.03 eV bands are attributed to excitation of the triplet $^3(n_o3s)$ state from the C_s and C_2 conformations, respectively. Their energy separation of 0.22 eV corresponds well to the difference of 0.25 eV found by Giulliani *et al.* in their calculations of the vertical excitation energies of the $^1(n_o3s)$ state for both conformations. The above assignments also give a singlet-triplet energy splitting of 0.31 eV for the n_o3s configuration, a value which might be expected for a Rydberg state. The triplet $^3(n_o3s)(C_s)$ band is strongly excited in the (a) (and also (b)) threshold spectrum and the intensity ratio of the triplet C_s and C_2 bands is 15.5, while the width of the C_2 band is lower by a factor of 2.5. Indeed, comprehensive studies of the electron impact excitation of polyatomic organic molecules[26] indicate that the triplet states are likely to be strongly excited at threshold and also to support negative ion resonances in the near-threshold energy region. To further support our assignment, Fig. 2(a) compares also the present threshold electron spectrum with the $C_2H_3O^-$ (mass 43 amu)

TABLE I. Vertical excitation energies (in electronvolts) of the electronic states of tetrahydrofuran determined with an uncertainty of ±0.02 eV.

Present work EI			Giuliani *et al.*[b] C		Giuliani *et al.*[c] VUV abs.		
C_2	C_S	Tam and Brion[a] EI	C_2	C_S	C_2	C_S	Assignment
5.87							valence
6.03	6.25						$^3(n_o3s)$
6.35	6.56	6.57	6.357	6.608	6.3	6.6	$^1(n_o3s)$
	7.21	7.19	6.889–7.103	7.154–7.381		7.19	$^1(n_o3p)$
	8.1	8.03	7.474–7.859	7.724–8.103	7.483		$^1(n_o3d)$
8.53	8.74		8.335–8.496	8.584–8.751	8.515–8.557	8.652–8.719	$^1(n_o4d)$
	8.93		8.615–8.635	8.872–8.899		8.888–8.939	$^1(n_o5p)$
	9.15		8.715–8.850	8.965–9.081	8.875	8.991–9.024	$^1(n_o5d)$
	9.33				9.037	9.130	$^1(n_o6d)$
	9.52				9.143	9.164	$^1(n_o7d)$
9.92							

[a]Reference 13.
[b]Theoretical results from Ref. 11.
[c]Experimental results from Ref. 11.

negative ion band obtained in the studies of the dissociative electron attachment to THF molecules by Ibănescu *et al.*[27] The conformity between the two spectra may indicate that the negative ions are produced via a resonance which concurrently decays into the triplet $^3(n_o3s)$ state. The dissociative attachment processes in THF were identified by Ibănescu *et al.* as proceeding via Feshbach resonances. This opens the possibility of a Feshbach resonance, which decays to the $^3(n_o3s)$ triplet state by emission of very low energy electrons. It is of note that the calculations of Bouchiha *et al.*[16] of the electron inelastic cross sections in THF, although performed for the assumed C_{2v} point group of THF molecule, found core-excited resonances in the energy region above the inelastic threshold. An alternative possibility is a core excited shape resonance formed above but close to the excitation threshold and decaying to its parent triplet state with an autodetachment rate allowing for predissociation by a repulsive valence state in the dissociative electron attachment process.

The broad maximum in spectrum of Fig. 2(b) is fitted with the same number of excitation bands as that in spectrum of Fig. 2(a). The intensity ratio of the $^1(n_o3s)(C_s)$ band to that of the $^3(n_o3s)(C_s)$ is higher, when compared to Fig. 2(a). The 7.21 eV excitation band is now clearly resolved by the fitting procedure and is assigned to the n_o3p states following the earlier electron impact[13] and photoabsorption[11] studies. The two remaining spectra shown in Figs. 2(c) and 2(d), measured at higher E_r values, show a further increasing intensity ratio of the singlet $^1(n_o3s)(C_s)$ to the triplet $^3(n_o3s)(C_s)$ bands. Our fitting to the spectra shown in Figs. 2(c) and 2(d) reveals a new excitation band at 6.35 eV, which is placed below that of the $^1(n_o3s)(C_s)$. This band may be assigned to excitation of the $^1(n_o3s)$ state from the C_2 conformation of the THF molecule, taking into account the 0.21 eV difference between the vertical excitation energies for both conformations. This difference is in accord with that calculated by Giulliani *et al.*[11] for the $^1(n_o3s)$ state. The intensity ratios of the $^1(n_o3s)(C_2)$ to $^1(n_o3s)(C_s)$ bands in Figs. 2(c) and 2(d) spectra are close to 7.0, whereas the widths of the C_2 band is twice as low as that of the C_s band. It is of note that the much lower intensity of the $^1(n_o3s)(C_2)$ band prevents its uncovering in the fitting of the spectra shown in Figs. 2(a) and 2(b). The 5.87 eV band, which may be correlated with excitation of a valence state, contributes to both, the spectra in 2(c) and 2(d) and there is also an indication of a weak excitation process at even lower energy. The n_o3p band is now well developed in both spectra and its weak superimposed structure suggests contributions from more than one excited state. Further excitation bands are seen around 8.1 eV. The 7.21 and 8.1 eV excitation bands in the (b), (c) and (d) spectra may be associated with the triplet as well as singlet states. The vertical energies of the identified 3s excitation bands together with their assignments are listed in Table I and are compared (where possible) with the results of earlier electron impact[13] and VUV absorption[11] works.

Fig. 3 presents an energy loss spectrum measured in THF at $E_r = 10$ eV and a scattering angle $\Theta = 0°$, which favors excitation of the optically allowed states. It contains three intense excitation peaks of the $n = 3$ Rydberg states and above 8.3 eV weaker structures due to excitation of higher lying Rydberg states of $n \geq 4$. Below 6 eV, a weak signal is compatible with excitation of the triplet states. Moreover, in Fig. 3 the vertical excitation energies of the THF states obtained in the *ab initio* calculation by Giulliani *et al.*[11] are marked by bars. The first peak in the spectrum, due to excitation of the $^1(n_o3s)$ state,[10,13] is resolved in the fitting analyses into two excitation bands, whose positions and widths are in excellent agreement with that found for the $^1(n_o3s)(C_2)$ and $^1(n_o3s)(C_s)$ bands in the analyses of the energy loss spectra of Fig. 2. Their intensity ratio is 6.8, approximately equal to that found in spectra shown in Figs. 2(c) and 2(d). The shape of the $^1(n_o3s)$ peak is consistent with the corresponding VUV absorption band of THF, recorded by Giulliani *et al.*, which clearly shows transitions from the two conformations of THF. Comparison of the position of the second peak in the spectrum with the calculated vertical excitation energies of the singlet n_o3p bands[11] indicates that the excitation from the C_s conformation contributes substantially to the intensity of this energy loss peak. This is in accord with the *ab initio* calculations of Giulliani *et al.*, which predicted much lower oscillator strengths for transitions from the C_2 conformation than those from the C_s conformation. The third peak at 8.1 eV (Fig. 3) incorporates

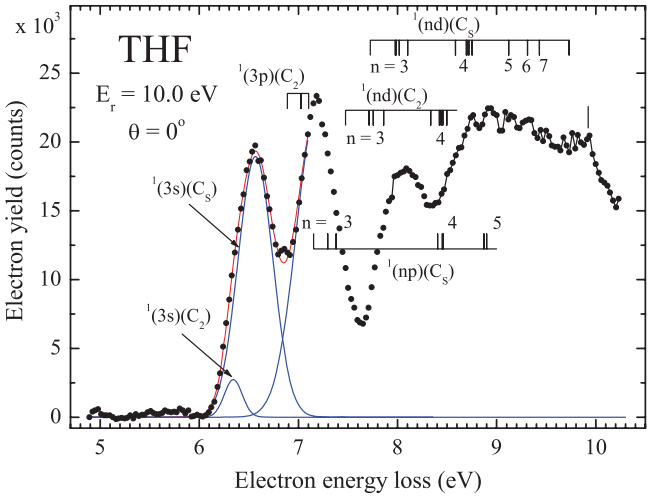

FIG. 3. Electron energy loss spectrum measured in THF for constant residual energy E_r of 10.0 eV and a scattering angle Θ of 0°. Also shown are (full lines) bands fitted to the $^1(n_o3s)$ peak and its final fit and the assignments of the bands for the C_2 and C_s conformations of the ground electronic state of THF. The vertical bars show vertical excitation energies from Ref. 11 of the indicated states of THF for transitions from the C_2 and C_s conformations.

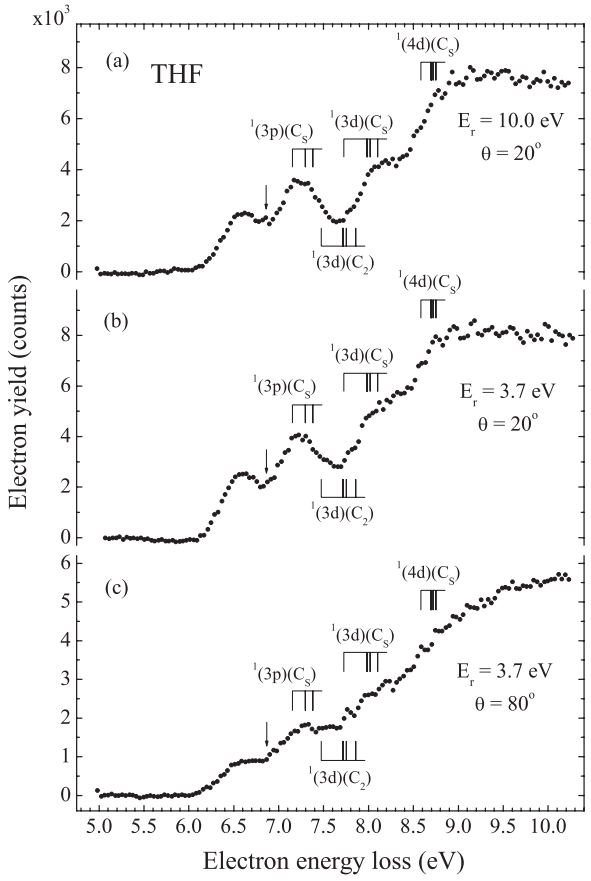

FIG. 4. Electron energy loss spectra measured in THF for constant residual energy and the scattering angle: (a) $E_r = 10.0$ eV, $\Theta = 20°$, (b) $E_r = 3.7$ eV, $\Theta = 20°$, and (c) $E_r = 3.7$ eV, $\Theta = 80°$. The vertical bars show vertical excitation energies from Ref. 11 of the indicated states of THF for transitions from the C_2 and C_s conformations of the ground electronic state of THF.

excitation bands of the n_o3d states.[11,13] The predicted vertical energies[11] of the $^1(n_o3d)(C_s)$ bands match well the positions of the weak structure at the top of the peak, while those of the $^1(n_o3d)(C_2)$ bands appear on the rising slope of the peak. This again may point to higher contributions from the C_s bands into the excitation transitions. It is interesting to note that the 9b/12a′ (C_2/C_s) photoelectron band,[28] which corresponds to the ion-core supporting the diffuse 3d Rydberg orbital, takes its intensity from ionization of the C_s conformation of THF, while ionization from C_2 conformation produces narrow vibrational structure on the rising slope of the total band.

In the assignment of the higher lying peaks in Fig. 3 to possible Rydberg states it is assumed, following the n_o3d excitation, that the C_s bands will appear with higher intensities in the energy loss spectrum than those of the C_2 bands. Thus, we interpret the 8.74 eV peak as corresponding to the $^1(n_o4d)(C_s)$ bands on the ground of coincidence with their calculated vertical excitation energies.[11] The $^1(n_o4d)(C_2)$ states are predicted above 8.3 eV in the calculations[11] and there is a weak structure on the rising slope of the spectrum at 8.53 eV. The energies of the higher states in the $^1(n_ond)(C_s)$ series were found using the Rydberg formula and the quantum defect $\delta = 0.293$, determined from the energy (8.74 eV) of the n = 4 state. The vertical ionization energy of 9.73 eV for the C_s conformation is taken from Ref. 28. The energies of 9.12 eV (n = 5), 9.31 eV (n = 6), and 9.43 eV (n = 7) were obtained, which agree better with the positions of the observed peaks than the calculated values.[11] The 8.93 eV energy loss peak may be assigned to the $^1(n_o5p)(C_s)$ bands. The 9.92 eV peak is placed above the first ionization threshold. Table I compares the obtained excitation energies of the THF states with the theoretical and experimental results of the VUV absorption[11] work and earlier electron impact[13] studies.

Although the energy loss spectrum of Fig. 3 shows on the whole excitation of the singlet Rydberg states of THF the results of Fig. 2, in particular the observed scattered electron background, indicate that a number of the THF states are excited in the electron impact and only some are clearly resolved as bands in the spectra. To study this issue further we measured energy loss spectra in THF for various constant residual energies from 2.3 to 10.0 eV and scattering angles from 20° to 80°. Selected three spectra are shown in Fig. 4. The calculated energies[11] of the singlet Rydberg states are marked by bars. As seen from comparison of spectra shown in Figs. 4(a) and 4(b), the overall shapes and the relative intensities of the singlet n = 3 Rydberg states do not change appreciably, when reducing E_r from 10.0 to 3.7 eV at 20° (when the incident energy changes from 16–20 eV to 9.5–13.5 eV). However, an increase of the scattering angle from 20° to 80° at $E_r = 3.7$ eV reduces the intensities of the Rydberg states and reveals the smoothly increasing scattered electron intensity, which is most likely produced by excitation of the optically forbidden (triplet) valence and Rydberg states. This behavior of the energy loss spectra of THF was very recently also observed by Do *et al.*[14] in their measurements at 15–50 eV incident energy.

The spectra of Fig. 4 show structures in the energy loss bands, which clearly supports our discussion of spectrum

in Fig. 3. The 3p peak includes at least two excitation bands. Spectra (b) and (c) point at a weak excitation of the $^1(n_o3d)(C_2)$ bands, while all three spectra indicate excitation of at least two $^1(n_o4d)(C_s)$ bands. A low intensity structure at 6.85 eV, between the 3s and 3p peaks, marked by arrow and also seen in the spectrum of Fig. 3, may correspond to excitation of a valence state.

IV. CONCLUSIONS

We have studied the electronic states of THF by measuring electron energy loss spectra in the energy range 5.5–10 eV. For the studies of the threshold and near-threshold excitation the penetrating field technique was exploited in our modified crossed electron-molecular beam spectrometer. This technique enabled the observation of the excitation of the triplet $^3(n_o3s)$ Rydberg state of the THF molecule and the determination of its energy. The present studies also allowed the identification of the electronic excitation of THF from the C_2 and C_s conformers of the ground electronic state and show that transitions from the C_s conformer have higher excitation cross sections. It is hoped that the results of this work will contribute to spectroscopic studies of THF and stimulate theoretical works on electron THF molecule collisions.

ACKNOWLEDGMENTS

This work was carried out within COST Action CM0601 "Electron Controlled Chemical Lithography." It was supported by the Polish Ministry for Science and Higher Education under Contract No. 553/N-COST/2009/0.

[1]M. N. R. Ashfold, G. A. King, D. Murdock, M. G. D. Nix, T. A. A. Oliver, and A. G. Sage, Phys. Chem. Chem. Phys. **12**, 1218 (2010).
[2]O. Sorkhabi, F. Qi, A. H. Rizvi, and A. G. Suits, J. Chem. Phys. **111**, 100 (1999).
[3]M. Stenrup and Å. Larson, Chem. Phys. **379**, 6 (2011).
[4]P. Sulzer, S. Ptasińska, F. Zappa, B. Mielewska, A. R. Milosavljević, P. Scheier, T. D. Märk, I. Bald, S. Gohlke, M. A. Huels, and E. Illenberger, J. Chem. Phys. **125**, 044304 (2006).
[5]L. Sanche, Eur. Phys. J. D **35**, 367 (2005).
[6]L. W. Pickett, N. J. Hoeflich, and T.-C. Lin, J. Am. Chem. Soc. **73**, 4865 (1951).
[7]G. J. Hernandez, J. Chem. Phys. **38**, 2233 (1963).
[8]R. Davidson, J. Høg, P. A. Warsop, and J. A. B. Whiteside, J. Chem. Soc. Faraday II **68**, 1652 (1972).
[9]J. Doucet, P. Sauvegeau, and C. Sandorfy, Chem. Phys. Lett. **17**, 316 (1972).
[10]L. J. Bremner, G. Martin, G. Curtis, and I. C. Walker, J. Chem. Soc. Faraday Trans. **87**, 1049 (1991).
[11]A. Giuliani, P. Limão-Vieira, D. Duflot, A. R. Milosavljević, B. P. Marinković, S. V. Hoffmann, N. Mason, J. Delwiche, and M.-J. Hubin-Franskin, Eur. Phys. J. D **51**, 97 (2009).
[12]V. M. Rayon and J. A. Sordo, J. Chem. Phys. **122**, 204303 (2005).
[13]W.-C. Tam and C. E. Brion, J. Electron Spectrosc. Relat. Phenom. **3**, 263 (1974).
[14]T. P. T. Do, M. Leung, M. Fuss, G. Garcia, F. Blanco, K. Ratnavelu, and M. J. Brunger, J. Chem. Phys. **134**, 144302 (2011).
[15]D. Antic, L. Parenteau, M. Lepage, and L. Sanche, J. Phys. Chem. B **103**, 6611 (1999).
[16]D. Bouchiha, J. D. Gorfinkiel, J. G. Caron, and L. Sanche, J. Phys. B **39**, 975 (2006).
[17]J. C. Gibson, R. J. Gulley, J. P. Sullivan, S. J. Buckman, V. Chan, and P. D. Burrow, J. Phys. B **29**, 3177 (1996).
[18]A. Gopalan, J. Bömmels, S. Götte, A. Landwehr, K. Franz, M. W. Ruf, H. Hotop, and K. Bartschat, Eur. Phys. J. D **22**, 17 (2003).
[19]I. Linert and M. Zubek, J. Phys. B **39**, 4087 (2006).
[20]S. Cvejanović and F. H. Read, J. Phys. B **7**, 1180 (1974).
[21]M. Zubek, D. S. Newman, and G. C. King, J. Phys. B **24**, 495 (1991).
[22]C. Schermann, I. Čadež, P. Delon, M. Tronc, and R. I. Hall, J. Phys. E **11**, 746 (1978).
[23]See http://www.electronoptics.com for information about the CPO programs.
[24]R. K. Nesbet, Phys. Rev. A **12**, 444 (1975).
[25]R. I. Hall, I. Čadež, C. Scherman, and M. Tronc, Phys. Rev. A **15**, 599 (1977).
[26]M. Allan, J. Electron Spectrosc. Relat. Phenom. **48**, 219 (1989).
[27]B. C. Ibănescu, O. May, and M. Allan, Phys. Chem. Chem. Phys. **10**, 1507 (2008).
[28]M. Dampc, B. Mielewska, M. R. F. Siggel-King, G. C. King, and M. Zubek, Chem. Phys. **359**, 77 (2009).